

Towards Modeling of Micro Breakdowns Observed in SEM

G. Damamme, N. Ghorbel,** G. Moya,* K. Zarbout**

Director of Research, CEA- Ile de France, 91310 Bruyeres- le-Châtel, France

Phone: 00330169267581, E-mail: gilles.damamme@cea.fr

*Professor, Université Paul Cézanne, 13397 Marseille, France

** Researcher, Université de Sfax, 3051 Sfax, Tunisie

Abstract – Breakdowns are the usual limitation of the dielectric using. The irradiation of materials by the electron beam of a scanning electron microscope can exhibit such breakdown events and also permit more elementary characterization of charging properties of non conducting materials. The physical mechanisms involved in such samples irradiated by defocused beams are investigated by combining some simple considerations of electron trapping mechanisms with an asymptotic analysis of the physics. This enables us to determine the electric field influence on mean free path. These elementary properties of dielectrics must be important to build up a model of micro breakdowns as observed under irradiation in a SEM. Other examples of electrical breakdowns as the ones of charged drops show that such instability phenomena are current and can oriented a physical modeling.

1. Introduction

The use of dielectric materials (ceramics, glasses, polymers) is limited by breakdown phenomena. Such phenomena can be extremely various in their physical mechanisms. Among the more frequent ones, we can suggest thermal breakdown caused by uncontrolled heating due to leakage current, or electron cascade process due to multiplication of ionization in field, or flashover on surface in void insulation.

Here we are more concerned by micro breakdowns as can be observed when an electron beam hits an isolating target. To progress with the understanding of such mechanisms and their physics, the irradiation of defocused beam (corresponding to a locally plane irradiation) is instructive and permits the determination of some elementary physical parameters.

2. SEM characterization

The electronic irradiation in a scanning electron microscope is considered as a privileged way to inject charges into insulators in a controlled manner. Thus, it is possible to estimate the trapped charge amount as well as its localisation in the sample (focused or defocused beam penetrating at different depths linked to primary energy E_p).

The subsequent events that occurred are somewhat complicated like that slowing down of the incident electron beam associated with the creation of electron-hole pairs (these carriers will be recombined or trapped on extrinsic or intrinsic sites).

Near the interface dielectric/vacuum, a part of electrons could escape leading to the secondary electron

emission (SEE). In consequence, the sample will present a trapped charge Q_T negative if fewer electrons escape than are been injected, or positive otherwise. Such evolution can be followed by monitoring the influence current I_{IC} in the metallic sample holder due to the charge image Q_{IC} effect (cf. Fig. 1).

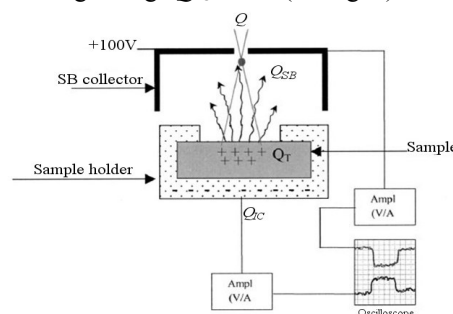


Fig. 1. Schematic view of the experimental apparatus in the SEM allowing to record the induced I_{IC} and secondary electron I_y currents. Q is the injected charge, Q_{IC} the induced charge, Q_T the trapped charge and Q_{SB} the secondary electron charge

The experimental setup is shown in Fig.1: the SEM apparatus is equipped with two complementary detectors surrounding the sample. The charge of true secondary and backscattered electrons Q_{SB} is collected on the SB collector, polarized at +100 V to ensure a good collection of secondary electrons, and measured through the current I_y . The charge remaining (trapped) in the insulator Q_T is determined through the induced charge present on the sample holder collector $Q_T = -Q_{IC}$. The charging experiments are carried out in the spot mode by focusing or defocusing the electron beam on the surface of the samples.

The evolution of the induced current $I_{IC}(t)$ as a function of the injected charge quantity $Q = I_p \cdot t_{inj}$ give us an interesting characterization of the material and of its near surface properties.

When focused beams are used, sometimes micro breakdowns appeared as peaks in the current $I_{IC}(t)$ (cf. Fig. 4 latter) which correspond to collective detrapping. On the other hand for defocused beam only smooth evolutions are observed which characterize not only the material but also the treatments submitted to the surface (e.g. polishing for glasses, etc.). In this case when specific representation of these evolutions is used, for example when the logarithm of SEE yield $y = I_y / I_p$ is plotted as a

function of the net trapped charge density Q_T/S , a very large range of linear dependency is observed (cf. Fig. 2 for MgO ceramic sample).

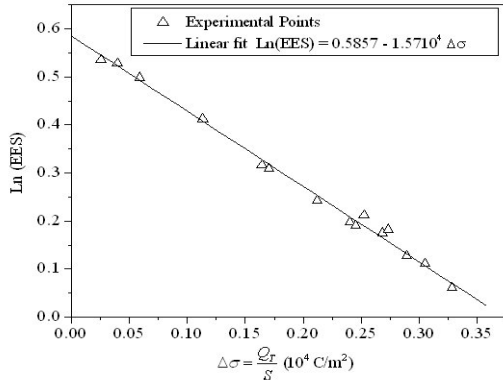


Fig. 2. Evolution of the SEE yield of MgO as a function of the trapped charge density

This behavior holds for different materials (MgO, Al_2O_3 , SiO_2 glasses) as well as different modes of elaboration of these specimens: single-crystals doped or not (cf. Fig. 3 for Cr doped alumina) and polycrystals (sintered alumina).

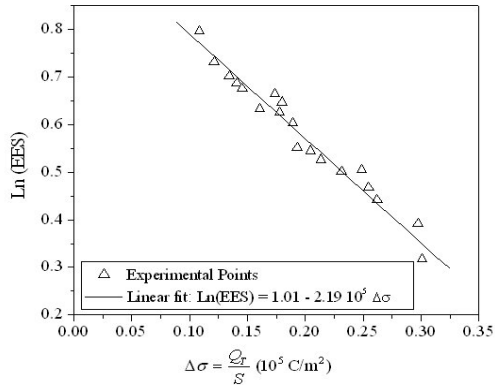


Fig. 3. Evolution of the SEE yield of Cr doped alumina as a function of the injected charge.

In the following section, we will show how a classical model of electron beam irradiation can explain such behavior, how it can be handled and which is the physical parameter obtained from the slope of such curve.

3. Modeling and Analysis of electrical phenomena under electron beam irradiation

The phenomena accompanying the electron/matter interactions are numerous and need a lot of parameters to be modeled. We use here one of the more simple version in the framework of the classical and simple model introduced by Fitting et al. [1, 2] a long time ago to tackle these phenomena.

Improvement and further developments could evidently be made but will not change the approach method and the main conclusions.

The slowing down of the incident electron flux j_0 is characterized by two functions, depending on the electron energy of the beam E_{cin} and the depth z .

The former $f(z, E_{cin})$ characterizes its lowering $j(z) = j_0 f(z)$ and the latter $g(z, E_{cin})$ the creation of electron-hole pairs $dn = j_0 g(z) dz$ (per unit of length).

The evolution (corresponding to thermalization and trapping) of the secondary electrons and of the holes is described by a two flux method (j_+ and j_- for the in and out coming flux, respectively) and characterized by their mean free paths λ_{\pm} which will depend on the electric field E and so will be different for the incoming and the outgoing components:

$\lambda_{\pm} = \lambda_0 \exp(\pm\beta E)$ where the quantities λ and β are naturally different for electrons (e) and holes (h) (β being of opposite sign). The corresponding balance equations are:

$$\pm \frac{\partial j}{\partial z} = S - \frac{j_{\pm}}{\lambda_{\pm}} \quad (1)$$

With $S_e = \frac{1}{2} j_0 \left(-\frac{\partial f}{\partial z} + g \right)$ and $S_h = \frac{1}{2} j_0 g$

The evolution of the trapped charge density resulting from the different flux is given by:

$$\frac{\partial \rho}{\partial t} = -\frac{j_{e+}}{\lambda_{e+}} - \frac{j_{e-}}{\lambda_{e-}} + \frac{j_{h+}}{\lambda_{h+}} + \frac{j_{h-}}{\lambda_{h-}} \quad (2)$$

The electric field $E(z)$ arise from the trapped charge $\rho(z)$ as well as the image charge created by the two interfaces (vacuum/dielectric and dielectric/metal). In fact, for a defocused beam, the charge distribution can be supposed locally plane as the one of the image due to the vacuum/dielectric interface.

Otherwise if the dielectric sample is thick enough (thickness e) in regards to the spreading of the implantation zone (surface S), the image due to the metal/holder interface can be supposed punctual. Thus the electric field expression is:

$$4\pi\epsilon_0\epsilon_r E(z) = \left(-\frac{1}{1+\epsilon_r} + \frac{\epsilon_r}{1+\epsilon_r} \frac{S}{(2e)^2} \right) Q_T + \int_0^z \rho(z) dz \quad (3)$$

If Q_T is important the surface potential V_0 can also modified the kinetic energy of the incident electrons E_{cin} as its flux j_0 . Then $E_{cin}(V_0) = E_{cin} + eV_0$ and $j_0(V_0) = j_0 \sqrt{E_{cin}(V_0)/E_{cin}}$.

Near the interface, the outgoing holes are completely reflected $j_{h+}(0) = j_{h-}(0)$, when the out coming electrons are partially reflected so constituting the secondary electron emission given by $SEE = \kappa j_{e-}(0)$, where κ is the transmission coefficient, and $j_{e+}(0) = (1-\kappa) j_{e-}(0)$.

Even in its simplest form, the modeling uses numerous hypothesis and parameters so that it is not easy to consider what are the pertinent or more fundamental ones. Furthermore the system of equations, even as simple as the previous one, can be resolved only by numerical simulation (cf. Fitting [1,2] and more recent papers [3,4]).

We will show that the consideration of the very different orders of length that arise in these experiments open the way to a powerful (although approximate) means of resolution and to a physical analysis of the phenomena.

4. Approach by matched asymptotic expansion methods

For incident electron energy of about ten of keV, the zone affected by charge accumulation is running to μm depth. Altogether the mean free path of electrons and holes is only about the nm and the source term of electron and holes is about one pair for nm length (when $j_0 = 1$).

So the problem introduces naturally two very different orders of length, the μm and the nm differing by a factor of 10^3 ; so the inverse will be taken, with ε , as very small quantities.

The equation where these quantities participate is given after renormalisation by ε :

$$\pm \varepsilon \frac{\partial j_{\pm}}{\partial z} = S - \frac{j_{\pm}}{\lambda_{\pm}}, \quad (4)$$

where all quantities evoked are now of the order of $O(j_0)$, the lengths being in μm .

This suggests tackle the problem by matched asymptotic expansion. Two different scales should be introduced, the exterior scale $x = z$ (range of μm) and the interior scale $\xi = z/\varepsilon$ (range of nm) which here will determine a boundary layer corresponding to the interface of the dielectric with vacuum. Each quantity (flux, charge density and field) possess now, an interior and an exterior development which comply with more simple equations than the initial ones and which match in the intermediate region (when $\xi \rightarrow \infty$ inner value equals outer value at $x = 0$). The full development is given by the sum of the two previous terms minus their common part:

$$f(z) = f(x = z) + f(\xi = z/\varepsilon) - f(x = 0 \text{ or } \xi = \infty) \quad (5)$$

Here $f(z)$, $f(x)$ and $f(\xi)$ are supposed to be different functions to have more simple notations.

Thus some consequences and simplifications can be obtained: flux in the exterior domain are now simply given by $j(x) = \lambda(E(x)) S(x)$ and in the boundary layer, even if the equation keep on to be complex, the source term $S(\xi)$ is now constant and equal to $S(z=0)$. Furthermore, the charge density ρ owns now two components, the first one (exterior domain) which complies with:

$$\frac{\partial \rho(x,t)}{\partial t} = -j_0 \frac{\partial f}{\partial z} \quad (6)$$

so that $\rho(x)$ is in $O(j_0 t)$

and the second (interior domain) corresponding to:

$$\frac{\partial \rho}{\partial t} = \frac{1}{\varepsilon} \left\{ -\frac{j_{e+}}{\lambda_{e+}} - \frac{j_{e-}}{\lambda_{e-}} + \frac{j_{h+}}{\lambda_{h+}} + \frac{j_{h-}}{\lambda_{h-}} \right\} \quad (7)$$

so that, within it, $\rho(\xi)$ is in $O(\varepsilon^{-1} j_0 t)$.

The variations of the field E are deduced from it and has a non trivial (i.e. non constant) fine structure $E(\xi)$ as a macroscopic one $E(x)$.

5. Results of the analysis

From the above hypotheses, the initial SEE yield can be analytically obtained in function of the kinetic energy E_{cin} of the incident electrons and is given by:

$$\frac{SEE}{j_0} = \kappa \lambda_{e0} S_e = \frac{1}{2} \kappa \lambda_{e0} \left(-\frac{\partial f}{\partial z} + g \right)_{(z=0; E_{cin})} \quad (8)$$

The pertinence of the evolution depends on the value taken for the mean free path λ , the transmission coefficient κ , the function $f(z, E_{cin})$ and $g(z, E_{cin})$. But more can be obtained analytically as the initial slope of the SEE yield in function of the trapped charge amount (by surface unit) since the initial flux $j(\xi)$, and evidently the flux $j(x)$, are particularly simple when no electric field is present.

Beyond some numerical evaluation must be made from:

$$j(0) \approx S_e(0) \lambda(E(0)) \approx S_e(0) \lambda_{e0} \exp(\beta E(0)),$$

where $E(z=0)$ is proportional to the trapped charge density via a numerical factor. Subsequently, we may write:

$$\ln(SEE) \approx \text{Cste} + \beta \cdot \text{coef } Q_T. \quad (9)$$

We note that the following relation (9) is confirmed experimentally (see Fig. 2 and Fig. 3) and the domain of precision is shown to be valid in a great range of charging effect by more precise calculations.

In ours experiments, where the direct effect of surface potential V_0 on the electron beam can be neglected (since V_0 is only about some volts) we are able to access directly from equation (9) to the important parameter β (the consideration of different incident electron energy could determine that effect independently).

Different materials have been characterized using this procedure. These results are reported in the Table I.

Table I. Some values of β coefficient for different materials

ceramic	Nature of the sample	β in m/V
MgO	Single-crystal	$3.3 \cdot 10^{-5}$
MgO	deposit layer	$2.2 \cdot 10^{-5}$
Al ₂ O ₃	Single-crystal doped with Cr	$2.7 \cdot 10^{-4}$
Al ₂ O ₃	sintered alumina	$5.2 \cdot 10^{-4}$

6. Extension of the approach

The modeling proposed for defocused beam can be extended. The difficulty is that the method of the two flux is only a good approximation in plane geometry; it became more fastidious (method with n flux) and approximate otherwise.

In experimental viewpoint, when we are proceeding with focused beams and using more important current density and more charge injection, micro breakdowns can then take place; then the influence current $I_{IC}(t)$

curves show peaks as illustrated in Fig. 4 for a charge injection realized on PMMA.

To progress in the micro breakdown physics, it can be interesting to consider other examples of electrical breakdowns. So, the one of the electrically charged droplet, in volume or in surface, gives a complementary look to the occurrence of catastrophic phenomena in connection with electrostatic. In these examples the limit charge is given in function of the radius of the drop and of its surface tension by exactly the same expression within a numerical factor.

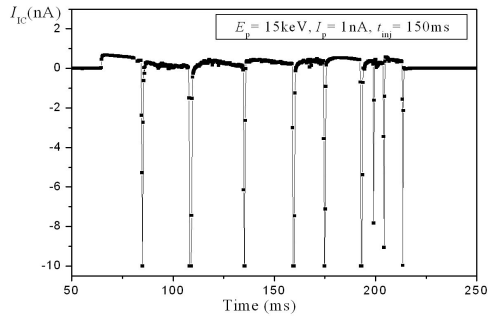


Fig. 4. Time-variation of the induced current $I_{IC}(t)$ during electron irradiation on PMMA (focused mode) at $E_p=15$ keV as primary beam energy and a fixed primary beam current ($I_p=1$ nA)

Altogether the nature of breakdown is very different in each case: separation in two droplets for the volume charge (it is the simple model of the liquid drop for the nucleus), ejection of an important part of the charge with a small fraction of fluid at the apexes of a bi conic configuration for the conducting liquid model (cf. Taylor [5]). What happens in micro breakdowns and collective charge detrapping could be nearer that second behaviour but the whole mechanism wait on for its description.

References

- [1] H.-J. Fitting, H. Glaefcke, W. Wild, R. Ulbricht, *Exper. Tech. Phys.* 24, 447 (1976).
- [2] H.-J. Fitting, H. Glaefcke, W. Wild, M. Franke, W. Muller, *Exper. Tech. Phys.* 27, 13 (1979).
- [3] I. A. Glavatskikh, V.S. Kortov, H.-J. Fitting, *J.A.P.*, 89 N°2, 440 (2001).
- [4] X. Meyza, D. Goeriot, C. Guerret-Piécourt, D. Tréheux, H.-J. Fitting, *J.A.P.*, 94 N°8, 5384 (2003).
- [5] G. Taylor, *Proceedings of the Royal Society of London, Series A: Mathematical and Physical Sciences*, 280, N°1382, 383(1964).